IIETA International Information and Engineering Technology Association
Advancing the World of Information and Engineering

Annales de Chimie - Science des Matériaux
Vol. 50, No. 5, October, 2026, pp. 425-434
Journal homepage: http://iieta.org/journals/acsm

Polyvinyl Alcohol Reinforced with Nano-Hydroxyapatite: Characterization and Mechanical Properties Improvement for Potential Artificial Intervertebral Discs Application

Noor A. Abduljawad*, Ahmed F. Hamzah

Department of Polymer Engineering and Petrochemical Industries, College of Materials Engineering, University of Babylon, Babylon 51001, Iraq

Corresponding Author Email: nen28820@gmail.com

Copyright: ©2026 The authors. This article is published by IIETA and is licensed under the CC BY 4.0 license (http://creativecommons.org/licenses/by/4.0/).

https://doi.org/10.18280/acsm.500501

Received: 12 June 2026
Revised: 29 July 2026
Accepted: 24 August 2026
Available online: 31 October 2026

Keywords:
polyvinyl alcohol, hydroxyapatite, citric acid, intervertebral disc replacement, composite biomaterials, mechanical properties, tissue engineering

ABSTRACT

Intervertebral disc degeneration (IVDD) is one of the leading causes of low back pain and spinal malfunction. Consequently, there is a need for materials that can restore the biomechanical performance and strength of the spine. This study aimed to design and analyze a composite based on polyvinyl alcohol (PVA) modified with citric acid (CA) and incorporating nanoparticles of hydroxyapatite (nHA) for possible utilization in intervertebral disc prosthetics. An aqueous solution of PVA at 20 wt.% was synthesized and modified using 10 wt.% CA. Hydroxyapatite nanoparticles at concentrations of 1 wt.% and 1.5 wt.% were incorporated into the PVA/CA matrix. Solution casting coupled with drying was employed to prepare the composite. The structural, physicomechanical, and biological properties of the composites were evaluated using X-ray diffraction (XRD), Fourier transform infrared spectroscopy (FTIR), scanning electron microscopy (SEM), tensile test, Shore hardness test, swelling test, density measurement, and 3-(4,5-dimethylthiazol-2-yl)-2,5-diphenyltetrazolium bromide (MTT) test. The results obtained by XRD indicated a decrease in crystallinity following CA incorporation. Also, FTIR spectra indicated intermolecular interactions and structural modification after incorporating CA. SEM images showed relatively homogeneous morphology with acceptable nanoparticle dispersion. It was shown that the hardness increased from 47.17 in pure PVA to 83.78 for PVA/CA/nHA with 1.5 wt.% of nHA. At the same time, the swelling ratio decreased from ~108% to 95%, and density increased from 1.2634 to 1.3304 g/cm³. Compared with PVA/CA, the tensile strength exhibited a slight increase with increasing nHA content. MTT Assay showed a concentration-dependent effect on cell viability of cells, where the viability of cells for human dermal fibroblast cells (HdFn) and MG-63 cells was 74.65% and 42.79%, respectively, at the highest concentration of 400 µg/mL. Overall, the PVA/CA/nHA composites showed enhanced hardness, decreased swelling, and a concentration-dependent effect on cell viability based on the MTT assay. It is clear that the developed materials can be further researched as possible candidates for intervertebral disc applications. Nevertheless, more biomechanical tests, such as compression, cyclic, fatigue, and shear tests, must be carried out in order to test their appropriateness for possible intervertebral disc replacement applications.

1. INTRODUCTION

The spine, otherwise referred to as the vertebral column, is a series of separated bones called vertebrae with intervertebral discs within which the spinal cord resides and extends down the back, connecting the head to the pelvis [1]. The intervertebral discs connect the vertebral bodies. They form one-third of the height of the spinal column and are the major joints. Due to the fact that they transfer loads that result from body weight and muscle activity throughout the spinal column on an ongoing basis, their main purpose is mechanical. They offer mobility for torsion, flexion, and bending [2]. The three main components of the intervertebral disc include the cartilaginous end plates, the annulus fibrosus, and the central nucleus pulposus surrounded by fibrous tissues [3]. As the major load-bearing and shock-absorbing element of the spinal column, the intervertebral disc is responsible for spinal flexibility and load transmission. It is thus clear that the functional mechanical properties of the spine depend directly on any injury or degeneration to the intervertebral disc (IVD). Injury to the intervertebral disc may facilitate degeneration and cause low back pain [4]. Discs moderately degenerated with some impairment are strongly associated with herniated intervertebral discs as well as various chronic pain disorders [5] that lead to further degradation and development of symptoms. The approaches to treatment include conservative therapy aimed at pain relief and not aimed at restoration of normal intervertebral disc function. Surgical treatments are

applied only to a small population and provide almost equivalent results. Generally, about 70–80% of all patients recover from their condition independently of the method chosen [2]. Nevertheless, the potential of innate regeneration in the intervertebral disc tissue is relatively low [6]. This makes the full restoration of disc properties difficult from the clinical point of view. Biomaterials intended for replacement of the intervertebral disc should have sufficient strength to bear physiological stress and pressures inside the intervertebral disc during everyday activity. In other words, there is a high need for biomaterials that will resemble the properties of natural tissue in regard to physiological conditions [7]. Polyvinyl alcohol (PVA) is considered to be one of the most extensively studied polymers for intervertebral discs due to its good physical characteristics, significant water content, mechanical properties, and biocompatibility [8, 9]. Nonetheless, PVA alone does not provide all necessary mechanical qualities to reproduce the mechanical behavior of natural intervertebral discs; therefore, it requires some reinforcing material. Hydroxyapatite represents a bioactive ceramic material, having a similar structure to bone minerals. The material has high biocompatibility and osteoconductivity, and it is successfully used for various biomedical applications due to its capability to facilitate cell attachment and tissue integration. In this paper, nanoparticle hydroxyapatite was chosen as a filler for reinforcement due to its nanostructure, providing greater surface area and better dispersion in the polymer matrix, which may lead to enhanced interfacial interaction and mechanical reinforcement [10, 11]. Although improvements in materials engineering and surgical technique have been made in recent years, currently existing solutions for intervertebral disc problems have not yet achieved a degree of functional recovery and regeneration of tissue in response to degeneration or disc herniation. On top of this, there are additional concerns related to these treatments since their risks include re-herniation, failure, and continued degeneration [7]. Artificial discs and spinal fusion products, despite being extensively researched, have not shown the ability to mimic the mechanics of natural intervertebral discs in cases of complex loading in the form of compression, bending, and shear, potentially leading to negative changes in spinal biomechanics [12]. Additionally, while several treatment methods such as discectomy, biomaterial implants, and cell therapy have been developed, their clinical success is inconsistent at best. While the intervertebral disc is constantly under pressure, cyclic loading, and multiaxial loads in the form of compression, bending, and shear, most of the existing implants are not equipped with enough fatigue resistance to endure these conditions. Poor long-term integration and material-tissue mismatch also contribute to poor performance and efficacy of existing treatment options. Therefore, current medical practice only manages pain rather than truly restoring function [13].

This study aims to synthesize and characterize the properties of PVA/citric acid (CA)/nanoparticles of hydroxyapatite (nHA) composites, thereby providing a preliminary evaluation of their potential for future uses as biomaterials for intervertebral discs.

2. MATERIAL AND METHOD

The PVA aqueous solution (PVA, Pallav Chemicals & Solvents Pvt. Ltd., Tarapur, India) was prepared by dissolving it to 20 wt.% concentration, then heating it up to 85 °C, stirring, until full dissolution. CA (10 wt.% of the total mass of the PVA solution) was added incrementally to the PVA solution through continuous stirring until full dissolution occurred. The nHA nanopowder (96% purity, average particle size of 60 nm, Hongwu New Material Co., China) was incorporated into the mixture at two different concentrations, 1 wt.% and 1.5 wt.%, which were based on the total mass of the PVA solution. The particles were previously suspended in deionized water using an ultrasonic bath to ensure proper dispersion. These solutions were cast into glass molds, the size of which was 10 × 20 cm with a thickness of 1 cm. The casting process lasted 7-10 days at room temperature to allow full drying of the samples. Then after that, they were demolded and cut to the required dimensions for further testing. All the tests were carried out at room temperature under laboratory conditions. Table 1 shows the composition of PVA composite samples.

Table 1. Formulation of polyvinyl alcohol (PVA) composite samples

Sample Code	PVA (g)	Water (g)	CA (g)	nHA (g)
Pure PVA	24	96	0	0
PVA/CA	24	96	12	0
PVA/CA/nHA 1%	24	96	12	1.2
PVA/CA/nHA 1.5%	24	96	12	1.8

Note: CA = citric acid, nHA = nanoparticles of hydroxyapatite.

3. CHARACTERIZATION TECHNIQUES

3.1 X-ray diffraction spectrum of pure polyvinyl alcohol and polyvinyl alcohol/citric acid mixture

The X-ray diffraction (XRD) spectra were obtained to determine the crystal structure of pure PVA and PVA/CA. Figure 1 represents the XRD spectra of PVA and PVA/CA. As shown in Figure 1, pure PVA possesses a sharp diffraction peak at $2\theta \approx 19.4°$, suggesting that it is semicrystalline. From the XRD analysis of the PVA/CA composite, there is only one broadened peak at a diffraction angle similar to that of pure PVA, with no noticeable peak shift. There is, however, a clear reduction in peak intensity and broadening. These results imply a decrease in crystallinity upon the introduction of CA into the sample, alongside an increase in the amorphous phase content. This could happen due to the effect of structural interaction between PVA and CA affecting the organized chain structure of the polymer [14].

3.2 Scanning electron microscopy analysis

Figures 2(a)-(c) show scanning electron microscopy (SEM) images of the PVA/CA/nHA composite at 500×, 1000×, and 2000× magnifications. As seen in Figure 2, the polymer matrix is relatively dense after the addition of CA. The bright spots represent the nHA particles in the polymer matrix. Nevertheless, certain clusters are observed as a result of interaction between particles. The surface morphology is relatively rough because of solvent evaporation during the drying stage, while the pores are minimal. There are no cracks seen, meaning that the composite remains structurally sound. Therefore, SEM results at various magnifications indicate a

relatively even distribution of nHA in the polymer matrix, though there is some agglomeration and unevenness observed. These results show that the inclusion of hydroxyapatite in the PVA matrix has been achieved successfully [15, 16].

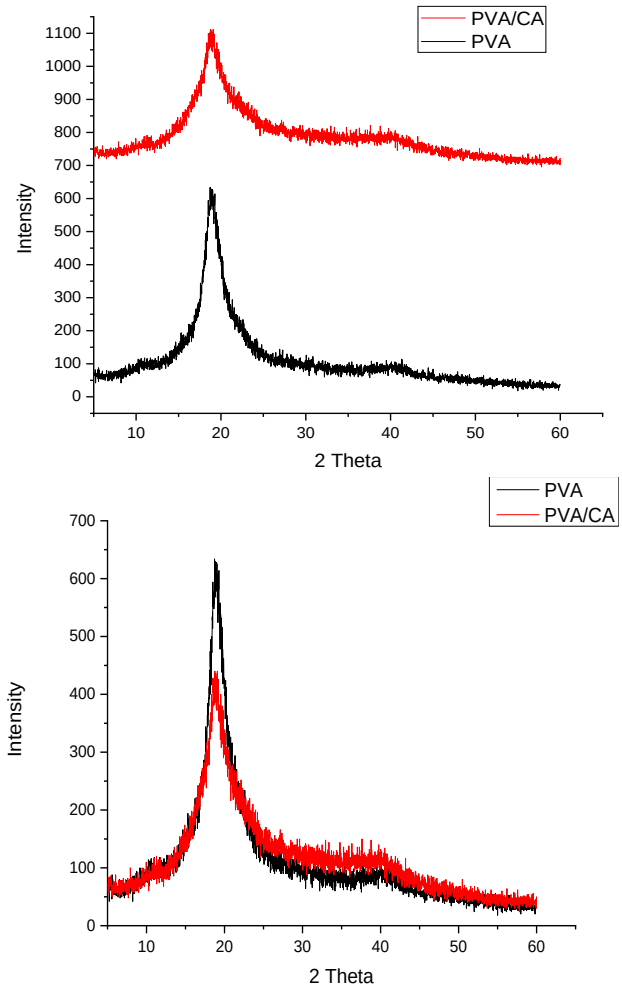
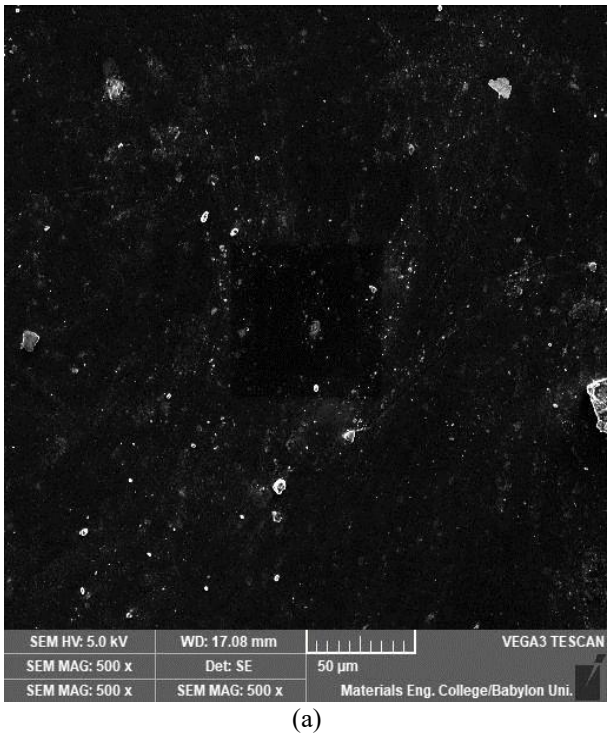
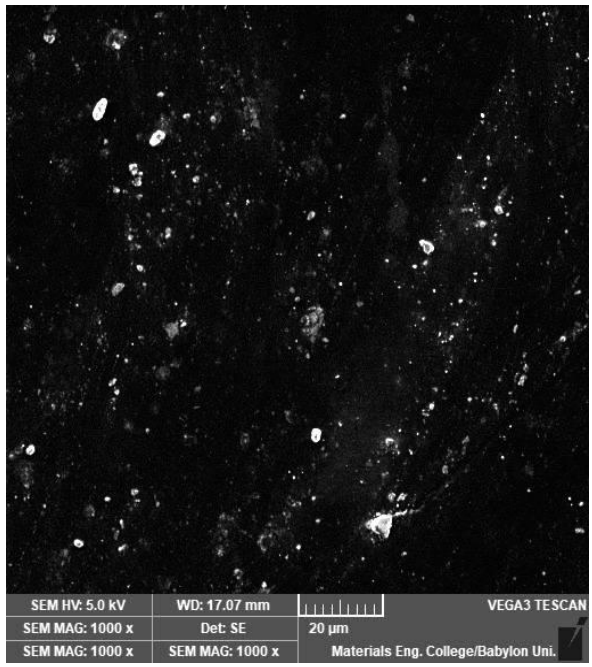


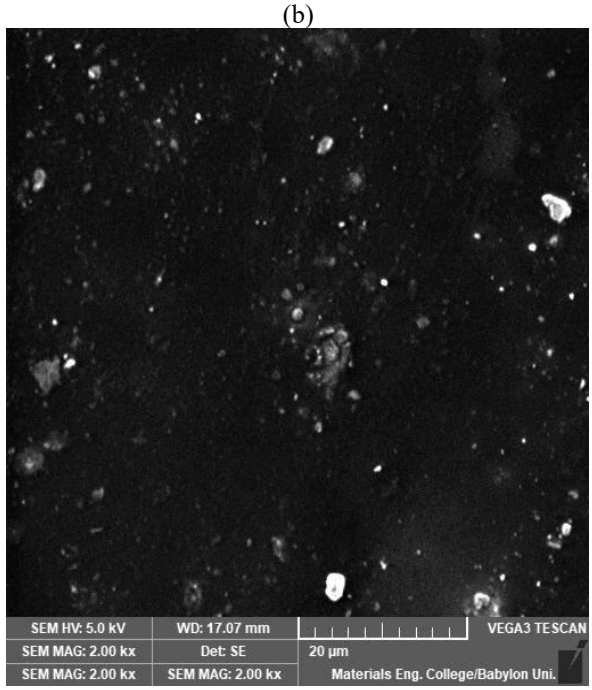
Figure 1. X-ray diffraction (XRD) spectra of polyvinyl alcohol (PVA) and PVA/citric acid (CA)



(a)



(b)



(c)

Figure 2. Scanning electron microscopy (SEM) of PVA/CA/nHA composite at different magnifications: (a) 500×, (b) 1000×, and (c) 2000×

Note: PVA= polyvinyl alcohol, CA= citric acid, nHA = nanoparticles of hydroxyapatite.

3.3 Hardness (Shore A)

According to the Shore A hardness test results, the hardness of the prepared samples increased gradually with the addition of CA and hydroxyapatite. Five hardness values were determined at various locations on each sample, and the data are presented in the form of mean ± standard deviation (SD). Pure PVA exhibited a relatively low hardness value of 47.17 ± 1.27, which can be attributed to its semi-crystalline structure and the high mobility of polymer chains. Upon the addition of PVA/CA, the hardness increased to 76.13 ± 1.10. This can be attributed to the limited mobility of polymer chains due to interaction between PVA and CA. The incorporation of 1%

nHA further increased the hardness to 78.08 ± 4.35, owing to the reinforcing effect of the ceramic nanoparticles. Increasing the nHA content to 1.5% resulted in a hardness value of 83.78 ± 6.29, indicating increased hardness and resistance to indentation. Figure 3 shows the Shore A hardness values of PVA and its composites in bar chart form [17].

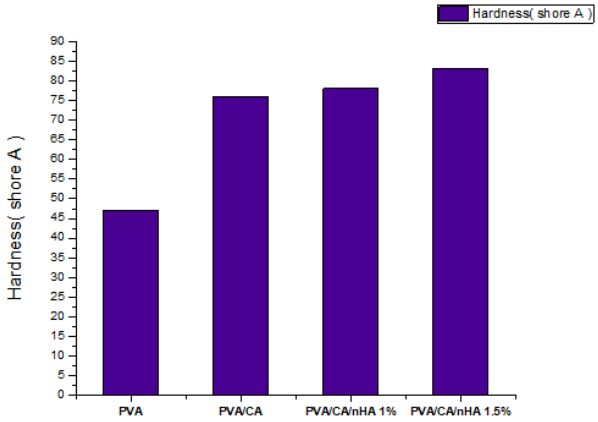


Figure 3. Hardness (Shore A) values of polyvinyl alcohol (PVA) and its composites

3.4 Swelling test

3.4.1 Preparation of the body simulation fluid (buffered phosphate-saline solution)

In order to create the buffered phosphate-saline solution, 9.88 g of BPS (Chemical Point Ltd., Weybridge, Surrey, UK) was dissolved in 1 liter of distilled water while being continuously stirred until the mixture was completely dissolved. After that, the solution's pH was brought to 7.4. After that, the samples' swelling behavior was assessed using the prepared solution. Every sample was submerged individually in separate containers filled with the buffer solution and allowed to sit in a controlled environment for a full day. The purpose of this process was to monitor and assess the prepared samples' swelling properties.

3.4.2 Swelling results

The prepared specimens were subjected to a swelling test using cut sections from tensile samples in order to verify dimensional uniformity and produce precise and comparable results. Before being submerged in the prepared medium for 24 hours, the specimens' weights and dimensions were measured. The weights and dimensions were measured once more after the surface water was carefully removed in order to assess the swelling behavior and related structural alterations.

The gravimetric method was used to assess the samples' swelling behavior. The following formula was used to determine the swelling percentage:

$$Swelling(\%) = \frac{W_s - W_d}{W_d} \times 100\% \quad (1)$$

where, W_d is the dry weight of the specimen before soaking, and W_s is the swollen weight of the specimen after soaking [18]. Table 2 shows the swelling behavior of pure PVA and its composite samples.

The pure PVA sample had the highest value for swelling percentage, which was 108%, because of the hydrophilic property of the pure PVA sample [18]. As seen in Figure 4, the use of CA decreased the swelling percentage to 101%. This decrease is attributed to restricted movement of the polymer chain and less free volume due to the interaction between PVA and CA [19]. Furthermore, the addition of nHA resulted in a further decrease in swelling (~95% at 1.5 weight percent and ~99.9% at 1 weight percent). This behavior is believed to be caused by the stiff ceramic particles that fill the gaps in the polymer matrix and restrict water absorption [20]. These findings show that the inclusion of CA and nHA resulted in reduced water uptake in the composite. Figure 5 shows an optical image of the sample before swelling compared with the specimen cut from the tensile test used in the swelling experiment.

Table 2. Swelling data

Sample	Dry Weight	Wet Weight	Swelling (%)
PVA	3.793 g	7.896 g	108%
PVA/CA	4.255 g	8.54 g	101%
PVA/CA/nHA 1%	3.55 g	7.098 g	99.9 %
PVA/CA/nHA 1.5%	5.370 g	10.445 g	95%

Note: PVA = polyvinyl alcohol, CA = citric acid, nHA = nanoparticles of hydroxyapatite.

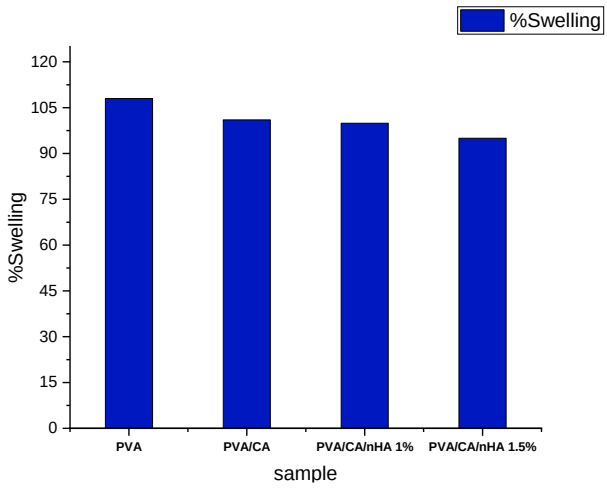


Figure 4. Swelling percentage of polyvinyl alcohol (PVA) and its composites



Figure 5. Optical image of sample before swelling compared with tensile cut mold

3.5 Density test measurement

Density measurements of the prepared samples were conducted using a high-precision density tester model GP-120 S (Matsu Haku, China) with digital resolution of ±0.0001 g/cm³, according to ASTM D792 [21]. Specimens collected from the tensile test after testing were used to measure their

densities. Each specimen was initially weighed in air, then submerged in distilled water at 23 ℃, using a sinker and wire to facilitate full immersion in the water during measurements. All specimens were first completely dried before testing to reduce any effects of moisture absorption while measuring. Density measurements were based on the principle of Archimedes, according to which the loss in weight of the body when it was submerged in a liquid equals the weight of the liquid displaced. Accordingly, the density of the specimen was calculated using the equation:

$$Density = Wair/(Wair - Wwater) * \rho fluid \quad (2)$$

where, $Wair$ is the weight of the specimen in air, $Wwater$ is the weight of the specimen immersed in distilled water, $\rho fluid$ is the density of the immersion liquid [22].

The findings showed a noticeable increase in the samples' density after CA was added; this may be attributed to structural modifications of the polymer matrix as well as reduction in internal voids [23]. Table 3 shows the density measurements of PVA and its composites.

Table 3. Density measurement

Sample	Density (g/cm³)
PVA	1.2634
PVA/CA	1.3076
PVA/CA/nHA 1%	1.3261
PVA/CA/nHA 1.5%	1.3304

Note: PVA = polyvinyl alcohol, CA = citric acid, nHA = nanoparticles of hydroxyapatite.

The samples' density gradually increased after nHA was added. The reason for this increase is that when nHA, a high-density ceramic material, is added to the polymer matrix, it fills in the gaps between the polymer chains and raises the overall density of the composite. This behavior also suggests a decrease in internal porosity and improved packing within the structure [11]. Figure 6 shows the density measurement of PVA and its composites in a bar chart form.

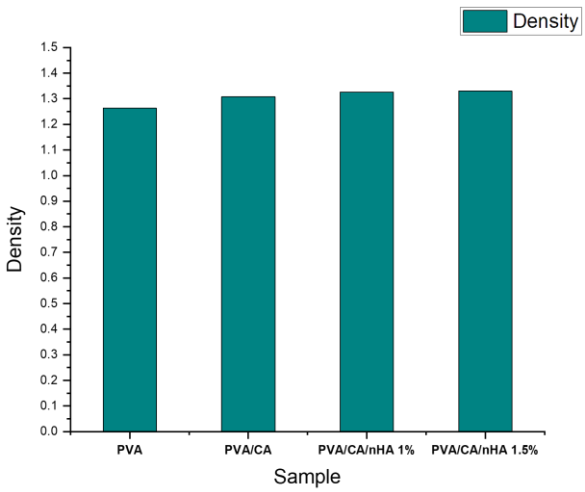


Figure 6. The density measurement of polyvinyl alcohol (PVA) and its composites

3.6 Tensile test analysis

The tensile test was conducted following the standard ASTM D638 [24] on a computerized universal testing machine (WDW-5E, China), which has a maximum load of 5 kN with a crosshead speed of 10 mm/min. The results presented here are the mean values of two specimens per formulation, and the test was performed at room temperature. Because there were just two samples tested per formulation, statistical significance analysis was not conducted. Hence, the tensile test results can only be regarded as preliminary and for comparative purposes only. The standard tensile specimen dimensions are shown in Figure 7.

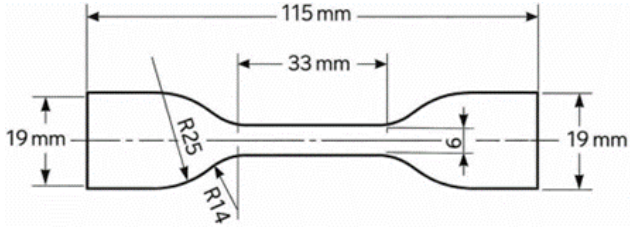


Figure 7. The standard sample dimensions

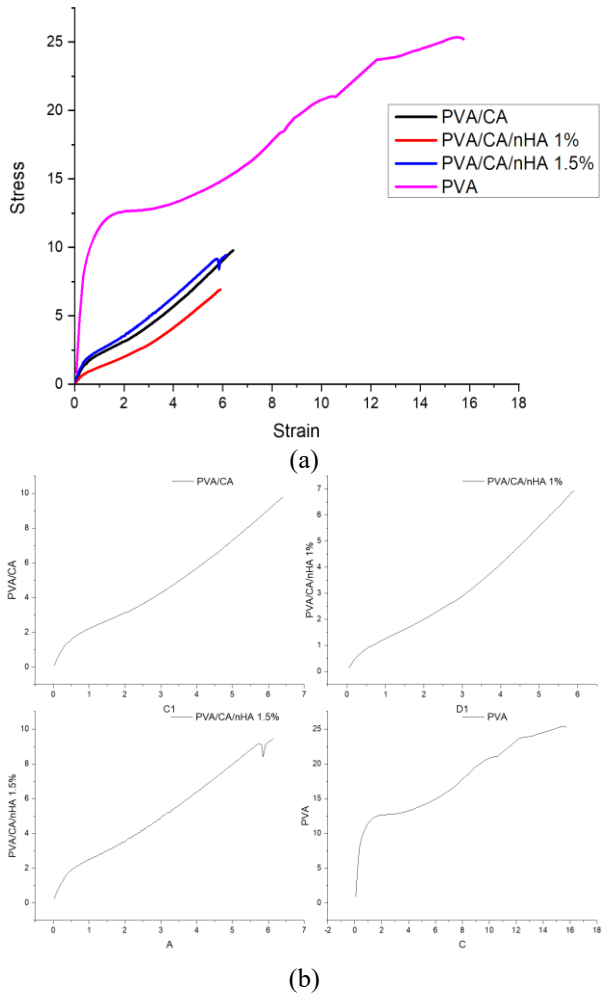


Figure 8. Stress versus strain graphs for pure polyvinyl alcohol (PVA) and its composite samples: (a) individual plots corresponding to each sample, and (b) combined plots showing all samples together for comparative purposes

The tensile test uses stress-strain curves to show how the various samples behave and how the addition of nHA and CA affects the mechanical characteristics of PVA, as shown in Figure 8.

The pure PVA sample initially displayed the greatest elongation at break and the highest stress values. Because of

the polymer's high molecular chain mobility and flexibility, which allow for significant deformation before failure, this behavior is expected. Consequently, this sample's behavior can be described as extremely ductile [25].

When PVA/CA was added, both tensile strength and elongation dramatically dropped. The reaction between PVA and CA can limit the movement of the polymer chain, which in turn makes the polymer less flexible [19]. When nHA was added at a weight percentage of 1%, tensile strength increased relative to the (PVA/CA) sample. The nHA particles may enhance load distribution and stress transfer by functioning as a reinforcing phase within the polymer matrix. Nevertheless, the elongation was still lower than that of pure PVA because of the restricted polymer chain movement resulting from the interactions between PVA and CA.

At a higher nHA content (1.5 weight percent), tensile strength increased even more, suggesting an enhanced ceramic phase reinforcement effect. However, Improvement in elongation was not observed, although it was rather limited. This suggests that increasing the filler content improves stiffness at the expense of ductility [26]. All things considered, pure PVA has a great deal of elongation and flexibility. Adding CA reduces ductility. Tensile strength slightly increased with the increase in nHA, while the elongation was still lower compared to pure PVA. The filler content and how it interacts with the polymer matrix determine the balance between stiffness and flexibility found in composite materials. The quantitative tensile properties of PVA and prepared composite specimens are tabulated in Table 4, which include tensile strength, maximum deformation, reduction in area, and elongation.

However, despite the enhanced stiffness obtained in these composites in relation to the amount of nHA incorporated, the mechanical evaluation carried out in the current research was limited to tensile testing. Moreover, only two specimens were subjected to testing for each composition, and hence there was no statistical analysis. The tensile testing results obtained cannot be used for prediction of the performance of these composite materials in application as intervertebral disc replacements since only tensile testing was carried out. Other mechanical tests such as compression, fatigue, cyclic, and shear need to be conducted.

Table 4. Tensile properties of PVA and its composites

Sample	Tensile Strength (MPa)	Maximum Deformation (mm)	Reduction of Area (%)	Elongation at Break (%)
PVA	20.0 ± 1.41	492.94 ± 101.07	56.25 ± 0.35	1408.5 ± 288.5
PVA/CA	7.5 ± 3.54	181.40 ± 64.82	59.25 ± 0.35	518.5 ± 185.3
PVA/CA/nHA 1%	7.5 ± 0.71	201.02 ± 11.23	62.50 ± 1.41	574.3 ± 32.2
PVA/CA/nHA 1.5%	9.5 ± 0.71	213.02 ± 9.75	63.25 ± 0.35	608.5 ± 27.6

Note: PVA = polyvinyl alcohol, CA = citric acid, nHA = nanoparticles of hydroxyapatite.

3.7 Fourier transform infrared spectroscopy characterization

To examine the chemical interactions and structural changes brought about by the addition of CA and nHA to the polymer matrix, the Fourier transform infrared spectroscopy (FTIR) spectra of pure PVA, PVA/CA, and PVA+CA+nHA (PVA/CA/nHA) composites were examined, as shown in Figure 9. The stretching vibration of hydroxyl (O-H) groups involved in intermolecular hydrogen bonding was represented by a broad absorption band in the spectrum of pure PVA at approximately 3200–3500 cm^{-1}. C-H stretching, C-H bending, and C-O stretching vibrations were identified as the cause of the distinctive peaks seen at roughly 2900–2940 cm^{-1}, 1427 cm^{-1}, and 1093–1143 cm^{-1}, respectively [27].

In the case of PVA after incorporation of CA, some changes were noticed in the FTIR spectrum. The broad –OH stretching peak was found to be weaker and also experienced a shift; this suggests the involvement of the hydroxyl group in intermolecular interactions and hydrogen bonding between PVA and CA. A peak at 1667 cm^{-1} has been observed, which can be attributed to the C=O stretching vibrations. The bands obtained at 1110 and 941 cm^{-1} may indicate C-O and C-O-C vibrations. The bands may indicate changes in the structure due to the addition of CA and intermolecular interactions in the PVA matrix. But these spectra alone cannot prove esterification and cross-linking chemically. The overall FTIR spectra revealed variations in the region of hydroxyl groups, carbonyl groups, and C-O/C-O-C bonds after the introduction of CA, indicating the interactions within the PVA matrix.

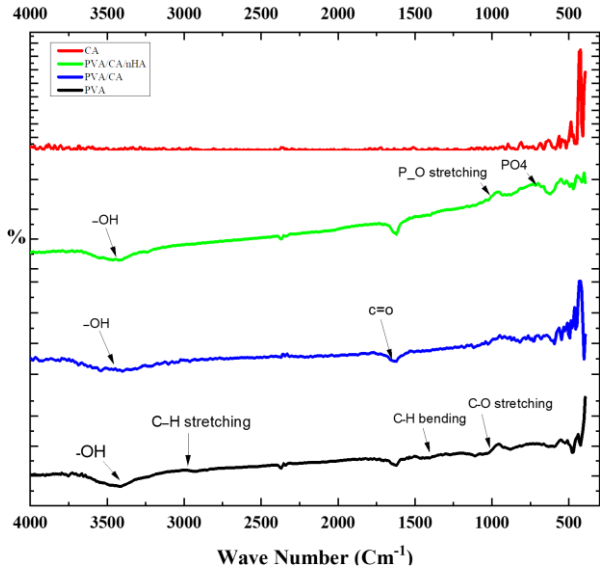


Figure 9. Fourier transform infrared spectroscopy (FTIR) spectra of PVA/CA and PVA/CA/nHA composites
Note: PVA= polyvinyl alcohol, CA= citric acid, nHA = nanoparticles of hydroxyapatite.

The changes in the spectrum indicate potential interactions between the esters and any modifications in the chemical environment of the PVA polymer after incorporation of the CA. However, it should be noted that the observed FTIR peaks might be due to hydrogen bonding, the presence of any CA, or other C-O/C=O vibration peaks [28-30]. For clarity, FTIR spectra for pure PVA and PVA/CA are also shown separately in Figure 10(a) and (b), respectively, whereby the distinct absorption bands and the variations of the spectra following

the addition of CA can be identified.

Further spectral changes were noted in the case of the PVA/CA/nHA composite, mainly in the 500-1100 cm^{-1} range. The bands present in this region are consistent with the presence of phosphate groups (PO_4^{3-}) associated with nHA in the polymer matrix. The existence of these vibrational frequencies, together with those of the hydroxyl, agrees with the use of nHA within the PVA/CA composite [27]. In general, the results obtained from the FTIR analysis demonstrate the presence of nHA within the PVA/CA mixture and suggest intermolecular interactions between PVA and CA. These findings are in line with the idea of chemical modification, but the FTIR analysis cannot be used to prove this.

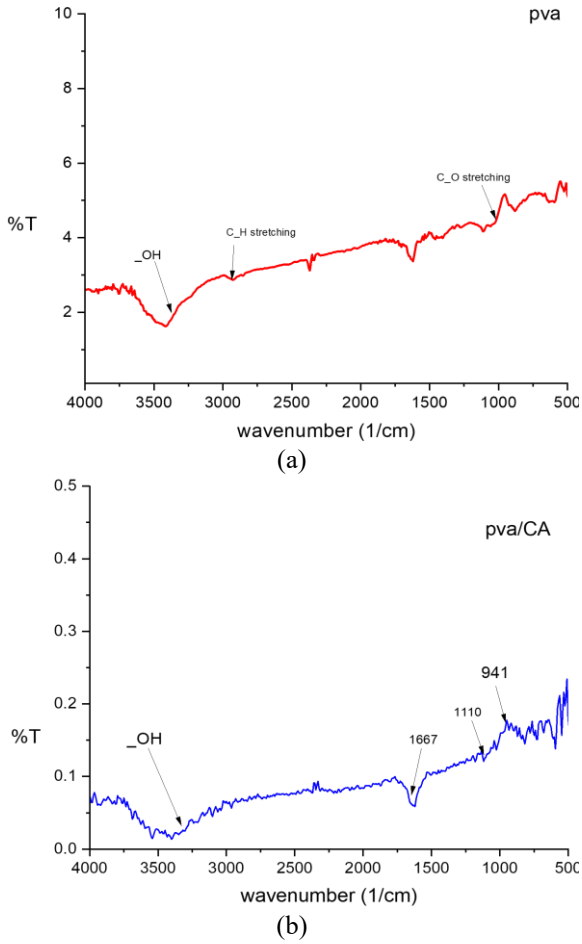


Figure 10. Fourier transform infrared spectroscopy (FTIR) spectra: (a) polyvinyl alcohol (PVA), (b) PVA/citric acid (CA)

3.8 3-(4,5-dimethylthiazol-2-yl)-2,5-diphenyltetrazolium bromide assay

Cytotoxic activity was evaluated in the Department of Pharmacology, Faculty of Medicine, Centre for Natural Product Research and Drug Discovery, University of Malaya, Malaysia. The cytotoxic potential of the final solid PVA/CA/nHA composite was examined on human osteosarcoma cells (MG-63) in comparison to normal control cells (human dermal fibroblast cells (HdFn)). The solid PVA/CA/nHA composite was used for the preparation of the test solution at concentrations of 25, 50, 100, 200, and 400 µg/mL. The test solutions were tested on MG-63 and HdFn cells that were grown in RPMI-1640 cell culture medium, with 15% fetal bovine serum (FBS), penicillin, streptomycin, sodium bicarbonate, HEPES, and L-glutamine added.

3-(4,5-dimethylthiazol-2-yl)-2,5-diphenyltetrazolium bromide (MTT) assay was performed using the MTT kit (Intron Biotech, Korea). Both cell cultures were grown in RPMI-1640 medium containing 15% FBS, penicillin, streptomycin, sodium bicarbonate, HEPES, and L-glutamine. Cultures were kept at 37 °C in a humidified air environment containing 5% CO_2. The cells were seeded in 96-well plates at a volume of 200 µL per well, and the process was followed by a 24-hour incubation allowing cell attachment. After that, the growth medium was replaced with various concentrations of prepared PVA/CA/nHA composite solutions (25, 50, 100, 200, and 400 µg/mL). For each concentration and control group, three wells were set up. Following 24 hours of exposure, 10 µL of MTT solution was introduced into each well, and the process was followed by a 4-hour incubation in the dark. Next, the medium was removed, and 100 µL of solubilization solution was added to dissolve the crystals. Absorbance was read at 575 nm using an enzyme-linked immunosorbent assay (ELISA) microplate reader. The MG-63 cell line was chosen as the osteoblast-like human cell line to perform the preliminary investigation on the cytocompatibility of the composite material, especially after the incorporation of nHA. The HdFn cell line was chosen as the normal human cell line.

The cell viability and cytotoxicity percentages were calculated according to the following equations [31]:

$$TestOD/ControlOD \times 100 = viability \quad (3)$$

$$Cytotoxicity = 100\% - Viability\% \quad (4)$$

OD means optical density.

Table 5 shows cytotoxicity assessment of PVA/CA/nHA composite against HdFn and MG-63 cells at various concentrations after 24 h of exposure.

Table 5. Cytotoxicity assessment of PVA/CA/nHA composite against HdFn and MG-63 cells after 24 hours of exposure

PVA/CA/nHA_24 h Concentration (µg/ ml)	HdFn (Mean ± SD)	MG-63 (Mean ± SD)
400	74.653 ± 0.703874	42.78533 ± 1.768329
200	88.65733 ± 2.253553	50.849 ± 1.771563
100	94.05867 ± 0.372318	63.81167 ± 3.04088
50	95.216 ± 0.240913	76.23467 ± 2.077898
25	95.949 ± 0.417273	85.60933 ± 2.645053

Note: PVA = polyvinyl alcohol, CA = citric acid, nHA = nanoparticles of hydroxyapatite, HdFn = human dermal fibroblast cells, SD = standard deviation.

3.8.1 Interpretation of polyvinyl alcohol/citric acid/nanoparticles of hydroxyapatite cytotoxicity results (24 h)

After 24 hours of treatment at various concentrations (25–400 µg/mL), the cytotoxic effect of PVA/CA/nHA composite on HdFn and osteosarcoma cells (MG-63) was assessed. The mean ± SD is used to display the results.

Overall, the viability of the two cell types decreased with an

increase in their exposure concentration to the PVA/CA/nHA composite. The calculated IC_{50} values for the MG-63 cells and HdFn cells were 94.53 µg/mL and 147.8 µg/mL, respectively as seen from Figure 11.

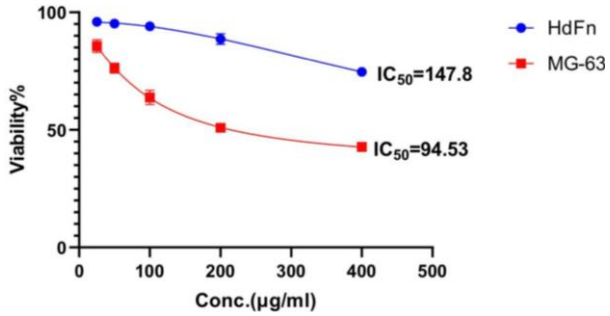


Figure 11. Dose-dependent effect of PVA/CA/nHA composite on the viability of HdFn and MG-63 cells after 24 h of exposure

Note: PVA= polyvinyl alcohol, CA= citric acid, nHA = nanoparticles of hydroxyapatite, HdFn = human dermal fibroblast cells.

The highest viability was seen in the group of cells receiving the lowest concentration of PVA/CA/nHA composite, which was 95.949 ± 0.417273 for HdFn cells and 85.60933 ± 2.645053 for MG-63 cells. When the dose increased to 50 and 100 µg/mL, a decline in cell viability occurred. For instance, at a concentration of 100 µg/mL, the viability of HdFn was 94.05867 ± 0.372318, whereas for the MG-63 cells it decreased to 63.81167 ± 3.04088. At this dose, MG-63 cells appeared to be more susceptible to the cytotoxic effects of the PVA/CA/nHA composite as compared to normal cells. At concentrations of 200 and 400 µg/mL, there was a cytotoxic effect of the PVA/CA/nHA composite on the two cell groups. The viability of HdFn and MG-63 cells was 74.653 ± 0.703874 and 42.78533 ± 1.768329, respectively [29].

4. STUDY LIMITATIONS

There are certain limitations associated with the present study. Although the fabricated composites exhibited promising performance in terms of their physical, mechanical, and biological properties, the mechanical characterization of the composite was limited to tensile and hardness properties. The compression, fatigue, cyclic load, and shear tests that need to be conducted for the application in the intervertebral disc have been neglected in this work.

One of the limitations of the current study is that the tensile test has been carried out using two samples for each composition, which would not be statistically validated due to the small sample size. The future study would incorporate more samples.

5. CONCLUSION

PVA/CA/nHA composites were fabricated and showed an increase in hardness and density, along with decreased swelling when compared to pure PVA. MTT assay served as an initial insight into the cellular response to the PVA/CA/nHA composite. With an increase in nHA content, hardness increased, accompanied by a slight improvement in tensile strength at 1.5% nHA. The synthesized composite could have potential to be explored further as a material candidate for the intervertebral disc.

Nevertheless, more biomechanical testing such as compression, cyclic, fatigue, and shear tests are needed before their suitability as intervertebral disc substitutes can be determined.

ACKNOWLEDGMENT

I thank the Deanery of the College of Materials Engineering for all their help during the research. I am thankful to my adviser, Dr. Ahmed Fadhil, for his valuable guidance and advice throughout the process. Additionally, I extend my appreciation to the administration of the College of Materials Engineering laboratory for their help in conducting experiments. Lastly, I would like to thank my family for their unending support and patience.

REFERENCES

[1] Frost, B.A. (2017). Polymer composite spinal disc implants. Doctoral dissertation, Virginia Tech. http://hdl.handle.net/10919/78783.

[2] Urban, J. P., Roberts, S. (2003). Degeneration of the intervertebral disc. Arthritis Research & Therapy, 5(3): 120. https://doi.org/10.1186/ar629

[3] de Almeida, P.L. (2021). Mimicking intervertebral disc mechanical properties with functionally graded auxetic composites. Universidade NOVA de Lisboa (Portugal). https://www.proquest.com/openview/8cc7e2a8648ac2bd6c3a52d82fe5903c/1?pq-origsite=gscholar&cbl=2026366&diss=y.

[4] Tavakoli, J., Diwan, A.D., Tipper, J.L. (2020). Advanced strategies for the regeneration of lumbar disc annulus fibrosus. International Journal of Molecular Sciences, 21(14): 4889. https://doi.org/10.3390/ijms21144889

[5] Yang, H., Liu, H., Li, Z., et al. (2015). Low back pain associated with lumbar disc herniation: Role of moderately degenerative disc and annulus fibrous tears. International Journal of Clinical and Experimental Medicine, 8(2): 1634. https://pmc.ncbi.nlm.nih.gov/articles/PMC4402739/pdf/ijcem0008-1634.pdf.

[6] Li, X., Dou, Q., Kong, Q. (2016). Repair and regenerative therapies of the annulus fibrosus of the intervertebral disc. Journal of the College of Physicians and Surgeons Pakistan, 26(2): 138-144. https://www.jcpsp.pk/archive/2016/Feb2016/15.pdf.

[7] Long, R.G., Torre, O.M., Hom, W.W., Assael, D.J., Iatridis, J.C. (2016). Design requirements for annulus fibrosus repair: Review of forces, displacements, and material properties of the intervertebral disk and a summary of candidate hydrogels for repair. Journal of Biomechanical Engineering, 138(2): 021007. https://doi.org/10.1115/1.4032353

[8] Paradossi, G., Cavalieri, F., Chiessi, E., Spagnoli, C., Cowman, M.K. (2003). Poly (vinyl alcohol) as versatile biomaterial for potential biomedical applications. Journal of Materials Science: Materials in Medicine, 14(8): 687-691. https://doi.org/10.1023/A:1024907615244

[9] Yang, M., Xiang, D., Chen, Y., Cui, Y., Wang, S., Liu, W. (2022). An artificial PVA-BC composite that mimics

the biomechanical properties and structure of a natural intervertebral disc. Materials, 15(4): 1481. https://doi.org/10.3390/ma15041481

[10] Mondal, S., Park, S., Choi, J., et al. (2023). Hydroxyapatite: A journey from biomaterials to advanced functional materials. Advances in Colloid and Interface Science, 321: 103013. https://doi.org/10.1016/j.cis.2023.103013

[11] Qiu, W., Wang, J., & Li, L. (2016). Preparation and biological performance of poly (vinyl alcohol)/hydroxyapatite porous composites used for cartilage repair. RSC Advances, 6(102): 99940-99947. https://doi.org/10.1039/c6ra22929h

[12] Denoziere, G., Ku, D.N. (2006). Biomechanical comparison between fusion of two vertebrae and implantation of an artificial intervertebral disc. Journal of Biomechanics, 39(4): 766-775. https://doi.org/10.1016/j.jbiomech.2004.07.039

[13] Buckley, C.T., Hoyland, J.A., Fujii, K., Pandit, A., Iatridis, J.C., Grad, S. (2018). Critical aspects and challenges for intervertebral disc repair and regeneration—Harnessing advances in tissue engineering. JOR Spine, 1(3): e1029. https://doi.org/10.1002/jsp2.1029

[14] He, Y., Zheng, Y., Liu, X., Liu, C., Zhang, H., Han, J. (2023). Polyvinyl alcohol–citric acid: A new material for green and efficient removal of cationic dye wastewater. Polymers, 15(22): 4341. https://doi.org/10.3390/polym15224341

[15] Wang, Z., Zhao, S., Hong, L., Huang, J. (2020). Preparation and properties of silver-based cellulose/polyvinyl alcohol antibacterial materials. Journal of Inorganic and Organometallic Polymers and Materials, 30(11): 4382-4393. https://doi.org/10.1007/s10904-020-01669-5

[16] Papapetros, K., Mathioudakis, G.N., Vroulias, D., Koutroumanis, N., Voyiatzis, G.A., Andrikopoulos, K.S. (2025). Structure-properties correlations of PVA-cellulose based nanocomposite films for food packaging applications. Polymers, 17(14): 1911. https://doi.org/10.3390/polym17141911

[17] Hervan, S.Z., Parlar, Z., Temiz, V., Altınkaynak, A. (2018). Friction and hardness characteristics of FDM-printed plastic materials. In Proceedings of 21st International Research/Expert Conference, pp. 65-68.

[18] Hu, X.L., Sun, C., Peng, B., et al. (2016). Swelling property of PVA hydrogels with different concentration and specifications and its influencing factors. International Journal of Clinical and Experimental Medicine, 9: 708-716. https://e-century.us/files/ijcem/9/2/ijcem0010778.pdf.

[19] Huang, S.M., Liu, S.M., Tseng, H.Y., Chen, W.C. (2023). Effect of citric acid on swelling resistance and physicochemical properties of post-crosslinked electrospun polyvinyl alcohol fibrous membrane. Polymers, 15(7): 1738. https://doi.org/10.3390/polym15071738

[20] Jalageri, M.B., Mohan Kumar, G.C. (2022). Hydroxyapatite reinforced polyvinyl alcohol/polyvinyl pyrrolidone based hydrogel for cartilage replacement. Gels, 8(9): 555. https://doi.org/10.3390/gels8090555

[21] de Oliveira Brito, M.T., do Nascimento Neto, P.F., Marinho França, R.J., Tinô, S.R.L., Fontes, R.S., Batista, A.C.D.M.C. (2023). Influence on mechanical properties with the addition of limestone powder in polyester/fiberglass composite. Journal of Composite Materials, 57(12) : 1989-1998. https://doi.org/10.1177/00219983231167215

[22] Salinas Domján, C., Valente, M., Romero, M.R. (2025). Mass density characterization of hydrogel-based systems inoculated with bacterial strains and dose-response performance of escherichia coli inoculation. Journal of Functional Biomaterials, 16(4): 121. https://doi.org/10.3390/jfb16040121

[23] Barandiaran, I., Gutierrez, J., Tercjak, A., Kortaberria, G. (2020). Effect of γ-Fe2O3 nanoparticles on the cross-linking and final properties of PVA/citric acid-based nanocomposites. The Journal of Physical Chemistry C, 124(9): 5444-5451. https://doi.org/10.1021/acs.jpcc.9b11219

[24] Raj, S.S., Kuzmin, A.M., Subramanian, K., Sathiamoorthyi, S., Kandasamy, K.T. (2021). Philosophy of selecting ASTM standards for mechanical characterization of polymers and polymer composites. Materiale Plastice, 58(3): 247-256. https://doi.org/10.37358/MP.21.3.5523

[25] Dai, Y., Tang, Q., Zhang, Z., et al. (2018). Enhanced mechanical, thermal, and UV-shielding properties of poly (vinyl alcohol)/metal–organic framework nanocomposites. RSC Advances, 8(67): 38681-38688. https://doi.org/10.1039/C8RA07143H

[26] Valarmathi, N., Sasikumar, K., Sumathi, S. (2021). In vitro biological activity of Zn substituted hydroxyapatite/polyvinyl alcohol composite for orthopaedic applications. Materials Today Communications, 26: 102025. https://doi.org/10.1016/j.mtcomm.2021.102025

[27] Zeng, S., Fu, S., Guo, G., et al. (2011). Preparation and characterization of nano-hydroxyapatite/poly (vinyl alcohol) composite membranes for guided bone regeneration. Journal of Biomedical Nanotechnology, 7(4): 549-557. https://doi.org/10.1166/jbn.2011.1316

[28] Hang, D.T., An, N.N.B. (2025). Enhancement of polyvinyl alcohol adsorbent via crosslink with citric acid and L-lysine for biochemical recovery from food processing waste streams. Journal of Science and Technology in Civil Engineering, 19(2): 92-106. https://doi.org/10.31814/stce.huce2025-19(2)-07

[29] Hussein, A.A., Kaddim Radi, N., Mohammed Sahi, N. (2025). Integrative computational and experimental study of propolis, polyvinyl alcohol, and alhagi maurorum complex as anticancer and antibacterial agents. Journal of Biomaterials Science, Polymer Edition, 36(12): 1718-1748. https://doi.org/10.1080/09205063.2025.2464448

[30] Pérez, G.B., Mendez, A., Ibarra, A.R., Monteiro, M., Ferreiro, O.B. (2025). Preparation and characterization of polyvinyl alcohol films crosslinked with citric acid and reinforced with microcellulose for controlled drug release. Materials Research, 28(Suppl 1): e20250131. https://doi.org/10.1590/1980-5373-MR-2025-0131

[31] Hasan, A.M., Majeed, S.M.A. (2024). Detection of anti-cancer activity of silver nanoparticles synthesized using aqueous mushroom extract of Pleurotus ostreatus on MCF-7 human breast cancer cell line. Iraqi Journal of Science, 65(4): 1886-1894. https://doi.org/10.24996/ijs.2024.65.4.9

NOMENCLATURE

CA	citric acid
FBS	Fetal bovine serum
FTIR	Fourier transform infrared spectroscopy
nHA	nanoparticles of hydroxyapatite
HdFn	human dermal fibroblast cells
IC_{50}	half-maximal inhibitory concentration, μg/mL
IVD	intervertebral disc
MG-63	human osteosarcoma cell line
MTT	3-(4,5-dimethylthiazol-2-yl)-2,5-diphenyltetrazolium bromide
OD	optical density, dimensionless
PVA	polyvinyl alcohol
PVA/CA	polyvinyl alcohol/citric acid system
PVA/CA/nHA	Polyvinyl alcohol/citric acid/nanoparticles of hydroxyapatite composite
RPMI-1640	cell culture medium used for MG-63 and HdFn cells
SD	standard deviation
SEM	scanning electron microscopy
T%	FTIR transmittance, %
W_d	dry weight of the specimen before soaking, g
W_s	swollen/wet weight of the specimen after soaking, g
wt.%	weight percentage, %
XRD	X-ray diffraction
BPS	buffered phosphate-saline

Greek symbols

θ	XRD diffraction angle, degree
μ	micro-prefix, 10^{-6}